



Review

How to design nanoporous silica nanoparticles in regulating drug delivery: Surface modification and porous control

Ruoshi Zhang, Ming Hua, Hengliang Liu, Jing Li^{*}

School of Pharmacy, Shenyang Medical College, Shenyang, China



ARTICLE INFO

Keywords:

Nanoporous silica nanoparticles
Drug delivery
Porous structure
Surface modification

ABSTRACT

Nanoporous silica nanoparticles (NSNs) have been considered with great interest as drug delivery agents owing to their superior properties. Herein, we review typical and recent progresses of NSNs, and for the first time, systemically pointed out the relationship between their formation mechanism, structure and regulation of drug delivery. Along with intelligent strategies of molecular/supramolecular switches and lipid membrane, NSNs greatly benefits from combination with molecular/supramolecular units as switches or from wrapping lipid membrane on their outside layer, which greatly improves regulation of drug delivery and therefore exert better efficacy of anticancer and other effects of the nanocomposite. It is expected that the review shall be of significance in designing NSNs as drug delivery systems with high efficiency and quality.

1. Introduction

Nanoporous silica nanoparticles (NSNs), defined as one kind of inorganic materials with nano pores (1–100 nm), possess not only common characteristics of being drug carriers like non-toxic, good biocompatibility and degradability, drug loading ability, but also unique advantages over other organic materials, including tunable particle size, rigid structure, facile functionality of internal and external surface area, etc [1–5]. It is widely accepted that the nanopores of NSNs can be divided into micropores (pore diameters of less than 2 nm), mesopores (pore diameters in the range of 2 to 50 nm) and macropores (pore diameters of greater than 50 nm) [6]. With the marriage of NSNs and pharmaceutical sciences, NSNs show abundant performances in a variety of drug delivery systems, mainly covering immediate drug delivery systems, sustained-release drug delivery systems, stimuli-responsive drug delivery systems and targeted drug delivery systems [7–13]. Hydrophobic drugs can be loaded into NSNs with enhanced drug delivery, which is recognized as an effective method to improve the low dissolution and bioavailability of poorly water-soluble drugs. The nanoscale of the pores and channels of NSNs also render their capacities to control drug release rate to perform sustained drug delivery effect. By using responsive functional groups, the drug molecules can only leak out when the established drug-loading system is exposed to external stimuli, including pH, redox potential, temperature, photoirradiation or enzymes, leading to stimuli-responsive controlled drug delivery. Apart

from the above advantages, NSNs are also effective in exerting rapid hemostasis and antibacterial activity, accelerating bone regeneration [90], detecting and adsorbing pesticide in agriculture field [91]. For example, tannic acid loaded mesoporous silica nanoparticles were established via covalent conjugation and electrostatic adsorption. The result showed that tannic acid loaded mesoporous silica nanoparticles could promote protein adhesion and favor the contact activation pathway of coagulation cascade with superior hemostasis [92]. Although there is a large number of papers report NSNs in different aspects, the in-depth relationship between the formation mechanism, structure and regulation of drug delivery has not been systemically discussed. It is no doubt that the mastery of it will be certain to provide a good foundation for designing NSNs with desirable characteristics and properties for regulating drug delivery (see Fig. 1), which belongs to one of our aims for producing this review.

In recent years, NSNs are experiencing their vital breakthroughs towards delicate and intelligent design, which can be mainly summarized into wrapping lipid membrane around NSNs [14–16] and installing molecular/supramolecular as switches onto the outer layer of NSNs [17]. NSNs wrapped with lipid bilayer membranes as drug carrier were first reported in 2011 [14], thus establishing “protocells” with core of drug loaded NSNs and shell of similar biofilm. In addition, molecular and supermolecular switches on NSNs have been paid great attention as the molecular/supramolecular switches turn out to be the cutting-edge research [17]. Thus, we give an overview on the application of NSNs

^{*} Corresponding author at: No. 146 Huanghe North Street, Shenyang, Liaoning Province, China.

E-mail address: dddefghijklmn@163.com (J. Li).

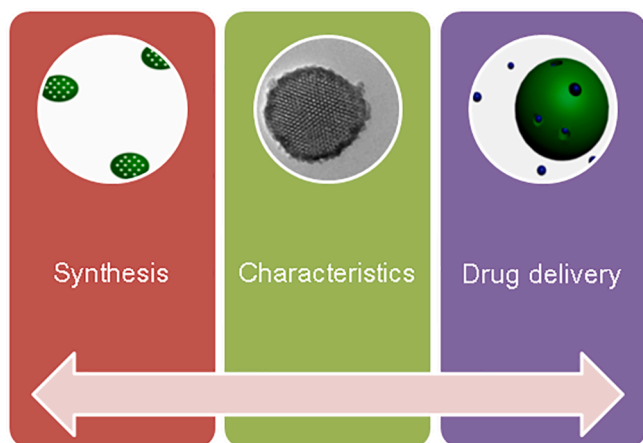


Fig. 1. Schematic diagram of the main contents that describe NSNs.

with lipid membrane wrapping and molecular/supermolecular switches in regulating antitumor drug on the basis of aforementioned relationship between structure of NSNs and their ability to regulate drug delivery. We could not deny that NSNs have shortcomings as follows, mainly including NSNs can not make sure: (1) precise pore size and particle size for all the NSNs; (2) accurate drug loading capacity in NSNs because a certain amount of drug molecules may adsorb onto the surface; (3) systemic safety in human body. It is believed that these shortcomings can be finally solved with the updating of research works and NSNs have promising value to be applied in many aspects.

2. NSNs

2.1. Synthesis of NSNs

2.1.1. Unmodified NSNs

The synthesis of NSNs bases on co-operative self-assembly of supramolecular surfactant that acts as structure directing agents [8,18]. As known, the formation mechanism of NSNs can be concluded into two main steps, which are hydrolysis and polycondensation. To be specific, silica source hydrolyzes to silicic acid, and these silicic acids condense to establish silica frame. The templates used in the system form micelles to direct the shape and pore size of silica [68]. Mesoporous silica nanoparticles (MSNs), belonging to NSNs, have been widely studied. Normally, there are several categories of MSNs, including Mobile Crystalline Material (MCM, such as MCM-41, MCM-48, MCM-50, etc.), Santa Barbara (SBA, like SBA-1, SBA-2, SBA-3, SBA-6, SBA-12, SBA-15, SBA-16, etc.), Hexagonal Mesoporous Silica (HMS), Michigan State University (MSU), Fudan University (FDU) and Anionic Surfactant Templated Mesoporous Silica (AMS). The critical point is to choose proper surfactant since different surfactants have various structures and charge properties. It is widely accepted that surfactants can be divided into four types according to charge property, which are cationic type (typical example is quaternary ammonium salt, like cetyltrimethyl ammonium bromide (CTAB), anionic type (compounds with carboxylic acid, phosphoric acid, sulphuric acid or sulfonic acid), non ionic type (like PEO-PPO-PEO) and ampholytic type. The synthesized routes can be different when using different surfactants. Herein, S^+ , S^0 , and S^- stand for cationic surfactant, neutral surfactant and anionic surfactant, respectively. Meanwhile, I^+ , I^0 , and I^- represent inorganic cations, neutral inorganic ions and inorganic anions. X^- is considered as Cl^- or Br^- , while M^+ stands for Na^+ or K^+ , etc. The description of synthesized routes of silica formation is given in Table 1, which assists to have a better understanding of the synthesized process.

With the abundant availability of various surfactants and facilely introduction of sol-gel chemistry, MSNs with different structures have been developed (see Table 2). Among them, MCM-41 is the most

Table 1
Synthesized routes of silica formation.

Surfactant	Synthesized route	Description	Represents
S^+	S^+I^-	Under alkaline condition, silicon species have negative electricity and form electrostatic interaction with cationic surfactant.	MCM-41, SBA-3
	$S^+X^-I^+$	Under acidic condition, silicon species have positive electricity and form electrostatic interaction with anion then with cationic surfactant.	
S^0	$S^0I^0 (S^0H^+)$	In the neutral medium, neutral silicon species form hydrogen bonding forces with surfactant.	HMS, MSU
	X^-I^+	In strong acid medium, the hydrophilic groups of surfactant connect with hydrogen ions to have positive charges. Silicon species have positive electricity and form electrostatic interaction with anion then with positively charged surfactant.	SBA-11, SBA-12, SBA-15, SBA-16, FDU-1, FDU-5
S^-	S^-I^+	Under acidic condition, silicon species have positive electricity and form electrostatic interaction with anionic surfactant.	AMS
	$S^-X^+I^-$	Under alkaline condition, silicon species have negative electricity and form electrostatic interaction with cation then with anionic surfactant.	

Table 2
Various mesoporous silica structures synthesized using different templates.

Mesostructure	Space group	Represents
Lamellar	–	MCM-50
Bicontinuous cubic phase	Ia-3d	MCM-48, FDU-5, AMS-6
	Pn-3m	AMS-10
	P6mm	MCM-41, SBA-15, SBA-3
2D hexagonal	Pm-3n	SBA-1, SBA-6
	Fm-3m	SBA-2, SBA-12
	Im-3m	SBA-16
	Fd-3m	FDU-2
	Unordered hexagonal	P6m

extensively researched type of mesoporous silica for biomedical applications [19–21]. With the surfactant of CTAB as liquid crystal template, TEOS or sodium metasilicate as the silica precursor, and alkali as catalyst, MSNs with ordered arrangement of 2D hexagonal mesopores were firstly synthesized and named as MCM-41. As an important member of MCM family, MCM-48 has also been paid attention and applied in drug delivery systems. MCM-48 with 3D bicontinuous structure belongs to the cubic Ia3d space group. Different from MCM-41 with unidirectional channels, MCM-48 with unique bicontinuous channels are favorable to achieve quick transport. Another widely researched type of mesoporous silica for drug delivery is SBA-15. SBA-15, with 2D hexagonal structure, was initially synthesized using amphiphilic triblock copolymer of poly(ethyleneoxide)-poly(propylene oxide)-poly(ethylene oxide) ($EO_{20}PO_{70}EO_{20}$, P123) as template in 1998 [22]. Generally, it has thicker pore walls and wider pore sizes (5 to 30 nm) than MCM-41 [22,23]. In addition, other types of mesoporous silica, such as MSU [24] and FDU [25] series mesoporous silica, also have great potential in biomedical applications.

Apart from single nanopore distributed NSNs, hierarchical NSNs with well-defined morphologies have been of growing interest, and a variety of templating approaches have been proposed to synthesize hierarchically nanoporous silica in the past decades. Bimodal nanoporous silica, including micro-meso, meso-meso, meso-macro, can be prepared using soft templates (such as colloidal particles, polymers, emulsion

droplets and surfactants, etc.) with abilities to form different sizes of nanopores [26–29]. The synthesized techniques for fabricating micro-meso silica include desilication method, hard template (such as carbon particles, ordered mesoporous carbon, carbon nanotubes, etc.) method, soft template method [30,31] and precursor assembly method [32]. Colloidal crystal template method, liquid template (emulsion, vesicles and bubble) method and biological macromolecule template method can be applied to prepare meso-macro silica. As for meso-meso silica, it is obtained owing to the dynamic templates originated from organic mesomorphous complexes or anionic surfactants.

Organic mesomorphous complexes of polyelectrolyte (such as poly(acrylic acid), PAA; polystyrene-*b*-poly(acrylic acid), PS*b*-PAA) and cationic surfactant (such as hexadecylpyridiniumchloride; CTAB) have been successfully applied to synthesize bimodal nanoporous silica [26–28]. It was reported that hollow carved mesoporous silica spheres were obtained using PAA and CTAB as dynamic templates. The silica precursors formed after silane hydrolysis co-assembled with CTAB micelles to form mesostructured silica. Meanwhile, PAA chains were extruded and phase can be separated from the PAA/CTAB complex, resulting in interstitial nanopores. Interestingly and importantly, a large number of secondary nanopores did not disturb the mesostructure of the mesoporous silica particles [28]. In the current stage, bimodal NSNs had been successfully synthesized using biomimetic method with C₁₆-L-serine as template [33]. Initially, C₁₆-L-serine forms micelle in aqueous solution because it consists of hydrophilic and hydrophobic ends on each side. The pH of system is adjusted to almost 13 because the alkaline environment purports transformation of C₁₆-L-serine between protonation and non-protonation. When 3-aminopropyl-triethoxysilane (APTES) and TEOS are added, the positively charged ammonium ion of APTES interacts with the negatively charged head group of hydrophilic part of C₁₆-L-serine through neutralization, which induces favorable electrostatic interactions [34]. The dynamic template can influence silica formation. APTES electrostatically interacts with template and meanwhile, the alkoxy silane sites of APTES are polymerized with TEOS to form silica framework. In this case, a certain amount of C₁₆-L-serine undergoes new dynamic self-assembly and TEOS accelerated the enlarged mesostructure formation of secondary larger nanopores. The study of hierarchical NSNs undoubtedly expands its profound application.

2.1.2. Surface modified NSNs

The silica surface consists of silanol groups, which can provide grafting sites for new comers. It has known that surface modified NSNs based on organosilanes can be commonly achieved by any of the following three methods, including co-condensation (one-pot synthesis), grafting (post-synthesis modification), and imprint coating method [1]. Co-condensation accomplishes the simultaneous hydrolysis and condensation of silica and organic silane in one-pot, while post-grafting finishes grafting of organic functional species on the surface after the synthesis of NSNs [9]. Co-condensation method is relatively superior owing to its relatively uniform distribution of the organic groups and higher loading of organic groups without closing the mesopores [35].

Herein, surface modified NSNs with 2D hexagonal structure is quoted as an example. In general, the anchoring of functional groups to the surface or opening sites as “gatekeeper” can be realized by grafting method. For example, NSNs were dehydrated under a nitrogen flow and then refluxed with APTES in toluene in order to graft amino groups to NSNs [21]. NSNs with gatekeepers of chemical entities (like nanoparticles, organic molecules, or supramolecular assemblies) on the opening sites construct stimuli-responsive systems. Short linker of disulfide bond is commonly applied to assist the grafting of various “gatekeeper”, including cyclodextrine and polyethylene glycol (PEG). In the synthesized procedure of PEG modified NSNs, 2,2'-dipyridyl disulfide was covalently bonded with thiol-functionalized NSNs to yield NSNs-SS-Py, which can further react with 3-mercaptopropionic acid to achieve NSNs-SS-COOH. Afterwards, the PEG chains were covalently

combined to NSNs-SS-COOH and thus obtaining the redox-responsive NSNs (NSNs-SS-PEG) [7,36]. A redox-controlled drug delivery system with aims for the development of site-directing and site-specific drug delivery system was studied. The system was comprised of a 3-(propyldisulfanyl) propionic acid-functionalized NSNs. The mesopores of this disulfide linker-NSNs were capped by 3-aminopropyltriethoxysilyl-functionalized magnetic iron oxide nanoparticles [12]. Poly(amido-amine) dendrimer was grafted onto NSNs via an isocyanatopropyl functionalized NSNs to alter the surface charge property of the capped mesoporous silica [37].

Co-condensation method is superior to grafting method due to its higher uniform dispersibility of functional groups. The conventional technique is to use silane coupling agent as co-structure directing agent. Recently, the co-condensation mechanism to get amino modified NSNs and carboxyl modified NSNs synthesized with respective templates of C₁₆-L-alanine and CTAB were intensively studied (Fig. 2) [38].

Two types of silane coupling agent were served as co-structure directing agent, and ion exchange method was employed to remove template at the final step. The weak base of ethanolamine was added to extract the template of amino modified NSNs. Thus, H⁺ originating from protonated amine was likely to be taken away by ethanolamine. Normally, anhydrous solvent, such as absolute ethyl alcohol, was applied in order to avoid the damage of silica frame. Similarly, dilute hydrochloric acid was mixed with extract liquor to extract the template of carboxyl modified NSNs. Under such circumstances, OH⁻ originating from unprotonated carboxyl was likely to be taken away by hydrochloric acid. Therefore, functional groups can be uniformly distributed after removing templates.

2.2. Fabrication of drug loaded NSNs

It is widely known that Vallet-Regi et al. initially proposed the use of NSNs as drug carriers by loading ibuprofen into MCM-41 and it opened up a new study era of NSNs. The nanoporous channels and pores of NSNs provide living space for drug molecules [39–42]. The loading of drugs into the NSNs has been generally carried out using organic solvent immersion, incipient wetness impregnation or the melting method. Drug loading process of NSNs by immersion can be described in the following three steps. Firstly, immerse NSNs into concentrated drug solution and fill the pores through capillary action. Secondly, diffuse drug molecules into the nanopores and adsorb them on the pore walls. Finally, recover the drug loaded NSNs from the solution. In an incipient wetness impregnation, a very concentrated drug solution is utilized to obtain a high loading degree because the drug concentration is usually close to its solubility. In this case, capillary action draws the solution as well as the drug molecules into the pores. In the melt method, a physical mixture of drug and NSNs is heated above the melting point of the drug. To some extent, this method can be considered as a special case of the impregnation method. Nevertheless, many drugs cannot withstand melting without degradation. In addition, high viscosity of the melted drug can be detrimental for successful drug loading.

Among these drug loading methods, solvent immersion method has been most frequently applied according to the literature [24,43–45]. For drug loaded NSNs using solvent immersion method, the polarity of the solvent can play an important role in influencing the drug loading. It is widely accepted that hydrogen bonding is a prevalent interaction between drug molecules and the surface of NSNs. Therefore, the favorable environment created by solvent for forming hydrogen bonding is very crucial. Very polar solvent, like dimethyl sulfoxide, can form competitive adsorption with drug molecules, causing a low degree of drug loading. The effect of solvent on the loading of poorly soluble drug ibuprofen has been systematically studied with dimethylformamide, dimethylacetamide, dimethyl sulfoxide, ethanol and hexane [10]. The result showed that almost no ibuprofen was loaded into MCM-41 with dimethylacetamide as solvent due to its extreme polarity. Nevertheless, the drug loading capacity with hexane as solvent increased to 37 wt%.



Fig. 2. Formation mechanism of surface modified NSNs with co-condensation method.

As for indomethacin, acetone was selected to be the solvent for loading drug into NSNs [43,46]. In consideration of the possibility of solvent residual and solvent safety, it is also acceptable to use relative safe solvents, such as ethanol [47]. Based on the above results from references, it was clear that the polarity of solvent can play an important role for achieving high drug loading capacity since hydrogen bonding between drug and carrier can be different in various solvent environment.

2.3. Influencing factors of regulating drug delivery

As stated above, NSNs have profound porous structures, rendering it possibility to present diverse drug release behaviors because the drug release rate in either channels or nanopores with various sizes and shapes will be different. Additionally, the silanol groups on the silica surface serve as adsorption sites for new comers [48]. The application of adsorption can be further expanded by introducing functional groups, such as weak acids (like carboxylic acids) and bases (like amines), onto the silica surface, which can be used to tune the surface charge under given pH conditions and provide the possibility for additional specific interactions [38]. With interactions between adsorbate and adsorbent, drug release behaviors can be affected at a certain extent. Therefore, surface modification of NSNs is emphatically focused apart from porous structure of NSNs regarding to its application in regulating drug delivery.

2.3.1. Porous structure

For unmodified NSNs, the initial noticeable impact of pores structure on drug release is its ability to entrap drug molecules so as to affect physicochemical characters of drug. In most cases, the small space of nanopores of NSNs restricted the crystal growth of drug molecules and impeded the existence of crystalline phase, resulting in the amorphous drug in NSNs. Such action significantly influences the delivery of poorly water-soluble drug, owing to the fact that conversion of drug crystalline state to amorphous phase can dramatically increase the apparent solubility of poorly water soluble drugs due to its higher energy state [49–52]. As seen in Table 3, the dissolution of amorphous simvastatin in mesocellular foam nanoparticles was more than 5 fold of crystalline simvastatin [42], and amorphous indomethacin in SBA-16 was higher than crystalline state of indomethacin. Generally for drugs belonging to BCS II, the enhancement of drug dissolution leads to improved drug

Table 3

Typical examples of the enhancement of poorly water-soluble drug dissolution using NSNs.

Ref.	Carrier	Template	Drug	Superiority
[41]	Mesoporous silica nanoparticles (MSNs)	CTAB	Telmisartan (TEL)	Its relative bioavailability was 154.4% ± 28.4%.
[42]	Mesocellular foam nanoparticles (MCF)	CTAB + PluronicP123	Simvastatin (SV)	During the same period, drug dissolution of SV-MCF reached 89%, while crystalline SV was only 17%.
[43]	SBA-16	CTAB + Pluronic F127	Indomethacin (IMC)	For crystalline IMC, only 64% of IMC was dissolved within 1 h. However, 75%, 81%, 90% of IMC being dissolved within 1 h for

bioavailability, typically as the relative bioavailability of telmisartan loaded MSNs was 154.4% ± 28.4%. The above results demonstrated that the successfully conversion of drug crystalline in the pores of NSNs to amorphous state contributed to achieve high drug dissolution and in vivo bioavailability.

On the basis of the conversion of drug crystalline state, the regulation of drug delivery depends on pore diameter of NSNs. The larger pore diameter, the faster drug dissolution rate and higher drug releasing amount. The accomplishment of silica condensation on different templates in the synthesized procedure leads to various porous structures, resulting in different pore sizes (Table 4). For example, CTAB can be used to fabricate MCM-41, and the addition of Pluronic F127 or Pluronic P123 as assistant template favors to form SBA-16 or SBA-15. Both SBA-16 with 3D cubic interconnected mesopores and SBA-15 with 2D hexagonal thicker wall have larger pore diameter than MCM-41, contributing to higher drug dissolution of carvedilol [39] and fenofibrate [40] than MCM-41, respectively. Fig. 3 vividly expresses the different drug release behaviors using these NSNs with various porous structures and

Table 4
The impact of pore diameter of NSN on drug delivery.

Ref.	Carrier	Structure	Template	Drug	Regulation of drug release
[39]	MCM-41	2D array with long 1D channels	CTAB	Carvedilol (CAR)	In simulated intestinal fluid environment, less than 20% of CAR was dissolved within 45 min for CAR crystals. More than 40% of CAR released from CAR loaded MCM-41.
	SBA-16	3D cubic interconnected mesopores	CTAB + Pluronic F127	CAR	More than 60% of CAR released from CAR loaded SBA-16 within 45 min due to larger pore diameter of SBA-16 than MCM-41.
[40]	MCM-41	2D array with long 1D channels	CTAB	Fenofibrate (FFB)	FFB loaded MCM-41 controlled drug release for 6 h.
	SBA-15	2D hexagonal with thicker wall	CTAB + Pluronic P123	FFB	FFB loaded SBA-15 showed burst release and sustained release for 4 h due to larger pore diameter of SBA-15 than MCM-41.
[52]	SBA-15	Pore diameter of 8.06 nm	Pluronic P123	AC	SBA-15 released 68% of drug at 45 min.
	MSF	Pore diameter of 24.48 nm	Pluronic P123	AC	After 45 min, MSF released 99% of its initial drug content.
[53]	B-CMS1	Pore diameter of 3.7 nm	C ₁₆ -L-alanine	IMC	IMC loaded B-CMS1 accomplished release at 90 min.
	B-CMS2	Pore diameter of 4.9 nm	C ₁₆ -L-alanine	IMC	IMC loaded B-CMS2 accomplished release at 60 min.
	B-CMS3	Pore diameter of 5.7 nm	C ₁₆ -L-alanine	IMC	IMC loaded B-CMS3 accomplished release at 20 min.
[33]	B-BNS	Small pore diameter of 7–8 nm Large pore diameter of about 30 nm	C ₁₆ -L-serine	Ibuprofen (IBU)	B-BNS regulated IBU release with two release phases. The small mesopores contributed to the first release phase in Simulated gastric fluid and burst

Table 4 (continued)

Ref.	Carrier	Structure	Template	Drug	Regulation of drug release
					release in simulated intestinal fluid. The large mesopores led to the second release phase in simulated gastric fluid and delayed release in simulated intestinal fluid.

pore sizes. The structures of MCM-41 and SBA-15 are both 2D hexagonal with space group of P6mm, and their differences are that the pore diameter of SBA-15 is larger and silica wall is thicker. Thus, drug releases faster from of SBA-15 due to its favorable space to escape from hexagonal array with long 1D channel. Regarding to the pore architecture, MCM-41 features hexagonal pores in a 2D array with long channels (P6mm group), while SBA-16 possesses a 3D cubic arrangement of spherical mesopores (Im-3 m group). It seems plausible to expect that the 3D structure of SBA-16 will provide more favorable drug release kinetics, while MCM-41 might exhibit sterical hindrance caused by the long pore channels [43].

With the same template of Pluronic P123, porous structure of NSNs can be controlled by adding swelling agent 1,3,5-trimethylbenzene in the reaction medium [52]. The introduction of 1,3,5-trimethylbenzene enlarged the pore diameter to 24.48 nm and induced the formation of MSF while the pore diameter of SBA-15 without pore enlargement was only 8.06 nm. After incorporating atorvastatin calcium into MSF and SBA-15, drug dissolution of atorvastatin calcium loaded MSF reached to 99% while atorvastatin calcium loaded SBA-15 released only 68%, confirming that the pore diameter of NSNs have direct and positive correlation with drug dissolution. The larger pore size of carrier, the higher drug dissolution because enlarged pores were favorable for the wetting of loaded drugs and further release. Applying the same template but slightly different synthesized conditions, porous structure of NSNs can be subtly controlled, which also regulates drug delivery. Hu et al. [43] prepared three types of SBA-16 that the silica condensed at temperatures of 80, 120 and 150 °C, which named S16-80, S16-120 and S16-150, respectively. The cage-like cubic phase of the S16-80, S16-120 and S16-150 with space group of Im-3m had pore diameters of 4.3, 6.8 and 9.0 nm. Comparing the dissolution of indomethacin from SBA-16, it revealed that the indomethacin dissolution behavior was mainly influenced by the pore diameter. Enlarging the pore size of SBA-16 from 4.3 to 9.0 nm significantly improved the indomethacin dissolution rate (Table 3). For S16-80 synthesized at low temperature, the relatively small cages and tight windows between these cages hindered the rapid drug diffusion into the media. In the meanwhile, the relatively larger pores of S16-150 synthesized at higher temperature with open and accessible surface area were more resistant to pore blocking and able to reduce the chance of restricting drug diffusions in the multidirectional pore system, thus allowing a faster drug dissolution. Li et al. [53] reported biomimetic synthesized chiral mesoporous silica (B-CMS) for loading and releasing indomethacin. Three types of B-CMS with helical channels synthesized under various pH or stirring rate conditions were denominated as B-CMS1, B-CMS2 and B-CMS3, and their pore diameters turned out to be 3.7, 4.9 and 5.7 nm, respectively. The results of in vitro drug dissolution (Table 4) confirmed again the ability of pore diameter in regulating drug release and drug dissolution rate was accelerated with enlarging the pore diameter of B-CMS. Interestingly, it has been reported that bimodal NSNs regulated drug release into two phases based on its double-stage mesopores [33]. The small mesopores (7–8 nm)

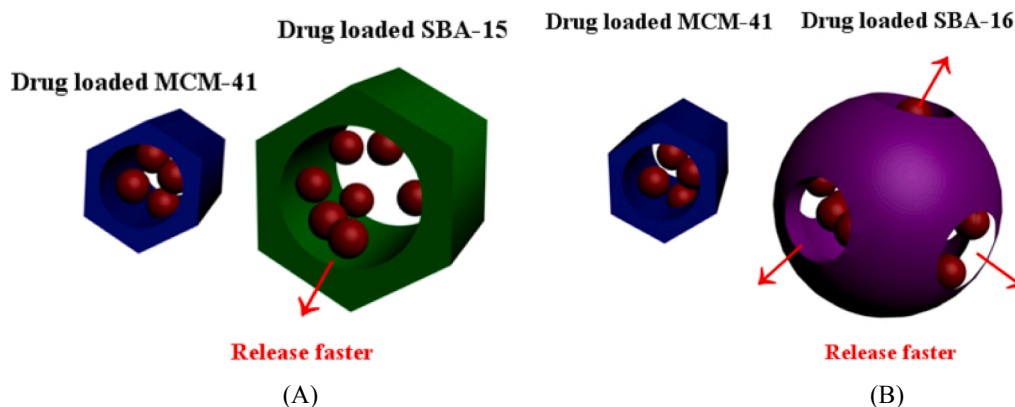


Fig. 3. Different drug release behaviors in these NSNs with various porous structures and pore sizes.

contributed to the first release phase in simulated gastric fluid and burst release in simulated intestinal fluid while the large mesopores (about 30 nm) led to the second release phase in simulated gastric fluid and delayed release in simulated intestinal fluid, reflecting again that the pore diameter of NSNs had strong impact on the drug delivery regulation.

2.3.2. Surface modification

On the basis of the silica frame of NSNs, if extra functional groups are endowed to the surface of NSNs, drug delivery can be regulated differently compared to unmodified NSNs (see Table 5). Among them, amino and carboxyl are the earliest studied functional groups for surface modified NSNs, which can largely change surface charges (positively charged of amino groups and negative charges of carboxyl groups) and pore structural parameters (lower surface area and pore volume). For surface modified NSNs with silica frame of ordered porous structure (2D hexagonal MCM-41) or unordered porous structure (unordered hexagonal MSU), the strong interaction forces formed between functional groups and drug molecules have the capacity to become the determined factor for regulating drug delivery. For example, the hydrogen bonding forces originating from either amidogen (amino modified MCM-41 and indomethacin [47]) or carboxyl group (carboxyl modified MSU and famotidine retarded drug release [24]) can prolong drug treating time at a certain extent because the formed hydrogen bonding delayed drug release rate. Apart from hydrogen bonding forces, hydrophobic interaction can also be the determined factor to regulate drug release [44]. The hydrophobicity of hydrophobic modified NSNs using co-condensation method can attract hydrophobic nimodipine strongly, thus slowing drug release.

In another aspect, the mutual responses formed between functional groups on the NSNs and external medium contribute to unpredictable drug delivery. For instance, hydrophobic modified NSNs using grafting method had selectively placed hydrophobic dimethylsilyl groups on the pore opening and external pore surface, and hence the hydrophobic surface of mesostructures retarded the penetration of solvents into the pore channels so as to delay drug release [54]. Another typical case of mutual responses of functional groups on the NSNs and external medium can be concluded as “stimuli-response” drug delivery system. It is widely accepted that any drug delivery system has to fulfill a list of desirable properties in order to achieve the release of the cargo in a suitable concentration at the desired target in a determined amount of time. NSNs based stimuli-responsive systems using a concept of gatekeeping were developed to achieve these goals. These systems have the advantage of using a variety of chemical entities (such as nanoparticles, organic molecules, or supramolecular assemblies) as “gatekeepers” to regulate the encapsulation and release of drug molecules [4,11,55–59]. This type of drug delivery systems with “zero premature release” performance is particularly useful when the cargo to be delivered is toxic,

like anti-cancer drugs. The obtained advantages of precise control over the location and timing of drug release would bring a major breakthrough to many site-specific delivery applications. These stimuli-responsive NSNs controlled release systems have real potential in achieving such an ambitious goal. There are several types of NSNs based nanodevices have been achieved through the development of photochemical, pH responsive, and redox active gatekeepers. Their capacities to regulate drug delivery are quite flexible and intelligent.

PEG-capped MSNs can be fabricated by taking advantage of disulfide bond. It was found that little amounts of rhodamine B released from M1-SS-PEG to the solutions in the absence of glutathione, demonstrating that the PEG-capped MSNs exhibited good capping efficiency. The rhodamine B release reached 40% at 10 h and 60% of the total rhodamine B at 24 h owing to the cleavage of the PEG gatekeepers at 10 mM glutathione. This M1-SS-PEG drug delivery system exhibited a sustained release manner because encapsulated drug molecules took a longer time to release due to PEG chains and interconnected pore networks of MCM-41 [7]. Poly(L-glutamic acid) (PLGA) is one of the widely studied synthetic polypeptides due to its modifiable carboxyl side group. The pH-responsive property ($pK_a \sim 4.5$) drug release of DOX@MSNs-PLGA was obviously pH dependent, and its dissolution increased with the decrease of pH. The cumulative release amount of DOX could reach up to 64% after 24 h at pH 5.5, which was much higher than that at pH 6.8 (28%) or pH 7.4 (13%). More PLGA would be protonated with decreasing the pH, thus making contribution in the dissociation of electrostatic interaction between PLGA and DOX and consequently more release of DOX. It was apparent that DOX@MSNs-PLGA performed superior pH-dependent drug dissolution than DOX@MSNs [60]. One recent work reported enzyme responsive NSNs by grafting multifunctional peptides GFLGR7RGDS. The in vitro release behaviors were investigated in PBS at a pH of 7.4 (physiological environment) and 5.0 (lysosome environment). In the presence of cathepsin B, about 60% DOX released from the DOX@MSN-GFLGR7RGDS/ α -CD nanoparticles while less than 10% DOX released in the absence of cathepsin B (20 U). This result indicated that cathepsin B can cleave the GFLG sequence and induce the removal of the gatekeeper from the surface of MSNs [11]. Based on above studies and in-depth discussion, it can be concluded that functional groups of NSNs influenced drug delivery regulation mainly by its interaction forces with drug molecules or outlet medium. Therefore, the efforts made in confirming and exploring of these interactions will certainly be efficient for us to develop surface modified NSNs with expected abilities.

2.3.3. Particle size

Particle size is an important influencing factor for nanoparticles because the nano size controls delivery route, such as the targeting site when circulating in vivo. As for NSNs, particles size is also crucial to affect drug delivery though not so many studies focused on this

Table 5
Different drug loaded surface modified NSNs.

Ref.	Carrier	Template	Drug	Regulation of drug release
[47]	Amino modified MCM-41	C ₁₆ TMABr	IMC	80% and 99% from amino modified MCM-41 and bare MCM-41, respectively in slightly alkaline medium.
[24]	Carboxyl modified MSU	C ₁₁₋₁₅ H ₂₂₋₃₀ (CH ₂ CH ₂ O) ₉ H	Famotidine (FMT)	The COO ⁻ -N ⁺ bondings formed between FMT and carboxylic groups in the mesostructure caused the delay of drug release rate.
[44]	Carbon chain modified macroporous silica spheres	PEO	Nimodipine (NDP)	Hydrophobic interaction between NDP and C ₈ groups on the carriers retarded drug release. The hydrophobicity of particles can attract hydrophobic NDP strongly, thus slowing drug release.
[54]	Hydrophobic modified mesoporous silica	CTAB	IBU	The hydrophobic surface of mesostructures retards the penetration of solvents into the pore channels, thus delaying drug release. The grafting modified materials, where the dimethylsilyl groups were placed selectively on the pore opening and external pore surface showed a long release compared to co-condensation method.
[7]	PEG modified MSN	CTAB	Rhodamine B (RhB)	Little amounts of RhB were released from M1-SS-PEG to the solutions in the absence of glutathione. Release of RhB reached 40% at 10 h and 60% of the total RhB at 24 h due to the cleavage of the PEG gatekeepers at 10 mM glutathione.
[60]	MSN with pH-Sensitive Nanovalves	CTAB	Doxorubicin (DOX)	Poly(L-glutamic acid) drug release rate of DOX@MSN-PLGA was obviously pH dependent and increased with the decrease of pH. The cumulative release amount of

Table 5 (continued)

Ref.	Carrier	Template	Drug	Regulation of drug release
[11]	Enzyme-induced MSN	CTAB	DOX	DOX could reach up to 64% after 24 h at pH 5.5, much higher than that at pH 6.8 or 7.4, which was 28% and 13%, respectively. In the presence of cathepsin B, about 60% loaded DOX has released from the DOX@MSN-GFLGR7RGDS/ α -CD nanoparticles incubated in pH 7.4 PBS buffer for 24 h. In contrast, in the absence of cathepsin B (20 U), due to the protection of the gatekeeper on the surface of the MSNs, less than 10% loaded DOX was released within the same time scale.

parameter. Normally, NSNs with particle size below 300 nm can be used in oral administration and injection route. It is not proper to apply NSNs with particle size larger than 300 nm for injection administration because large particle size can easily aggregate [8]. In general, small particle size of NSNs was favorable for achieving superior cellular uptake and therefore better delivery effect [83]. The particle size can be enhanced after capping guest molecules onto NSNs and thus delivery effect can possibly be a little different from unmodified NSNs [81]. Overall, particle size of NSNs has great effect on delivery route, including targeting site and in vivo distribution.

3. Design of NSNs for regulating drug delivery

The profound drug delivery regulation effect of NSNs enriches the application of inorganic porous materials in pharmaceutical sciences. In current stage, the study of NSNs normally focuses on the relationship between characteristics of NSNs and its application, just as most studies of drug carriers. While to be emphasized, it is equally crucial to figure out how synthesized conditions and process influence the formation of NSNs with properties to exert functions. The achievement of above relationship is able to promote the research to a higher level based on its great value in radically instructing the design of NSNs with expected properties and applications. The following contents in this section provided the description and discussion about this relationship, which has never been presented by any means elsewhere, making up this deficiency. Several typical synthesized conditions, including pH, stirring rate and temperature etc., were mainly addressed.

3.1. pH

In the synthesized system of NSNs, pH has a strong impact on cooperative self-assembly process of silica formation because the synthesized routes of formation mechanism (S^+I^- , $S^+X^-I^+$, S^0I^0 , $(S^+H^+)X^-I^+$, S^-I^+ , or $S^-X^+I^-$) can only work under a certain pH environment [61]. NSNs with various morphologies and porous structures can be obtained under various pH conditions. For instance, the isoelectric point of silica

is about 2 and silica species are protonated, and thus positively charged I^+ is at $pH < 2$ while negatively charged I^- is at $pH > 2$. Therefore, ordered mesoporous silica with differing mesostructures can be successfully synthesized using both cationic surfactants via S^+I^- and $S^+X^+I^-$ routes and non-ionic surfactants via S^0I^0 and $(S^0H^+)(X^-I^+)$ routes. However, only lamellar and disordered mesostructures have resulted from the use of anionic surfactants via conventional S^-I^+ or $S^-M^+I^-$ strategies as there are no critical interactions between surfactant head groups and silica source [61,62].

What is more, it is known that the self-assembly of anionic surfactant template silica complex can form a silica tropic liquid crystal phase depending on the lyotropic liquid crystal phases. Liquid crystal phases (bilayer, cylindrical and spherical) can normally be described using the surfactant packing parameter, $g = V/a_0l$, where V is the surfactant chain volume, a_0 is the effective hydrophobic/hydrophilic interfacial area, and l is the dynamic chain length. Based on the above geometrical relationships, bilayer, bicontinuous, cylindrical or spherical micelles can be formed when the g values reach to 1, 2/3, 1/2 and 1/3, corresponding to lamellar, 2D-cylindrical, bicontinuous (tricontinuous) minimal surfaces and micellar cage-type mesostructures, respectively (Table 6) [63]. Thus, pH conditions play crucial role in regulating mesostructures of anionic templated nanoporous silica by changing charging state of the surfactant, the area of the hydrophilic head and the average packing parameter. If APTES is used as the co-structure directing agent, the synthesis of anionic template nanoporous silica is more complicated. The pKb of APTES is about 3.4 caused by its amino groups. When we set molar ratio of co-structure directing agent / $-COOH_{(surfactant\ head\ group)}$ at 1, the surfactant head groups are almost all charged after the adding of acid. The opposite charges are expected to decrease the repulsion, leading to the low a_0 and high g values. When the environment was more acid ($HCl/-COOH_{(surfactant\ head\ group)} > 1$), the carboxylate groups of anionic surfactant can be protonated, resulting in high g value. Characteristics that include morphology and porous structure of NSNs can be adjusted by regulating g values.

Li et al. had systemically reported how pH influenced characteristics of NSNs and drug delivery behaviors [53]. Herein, biomimetic chiral mesoporous silica was synthesized using anionic surfactant of N-palmityl-L-alanine and co-structure directing agent of APTES. B-CMS1 and B-CMS2 were prepared in system environment of pH 11 and pH 13, respectively. As we know, surfactant packing is the dominant factor in determining the final structure of B-CMS, and the matching between the interfacial charge density of the surfactant head groups affects the kinetics of mesophase transition [64]. The formation of B-CMS can be successfully achieved under alkaline condition because the surfactant is anionic in the system. In this case, electrostatic interactions between surfactant and APTES are formed. B-CMS1 presented as many almost cocoon particles and the channels on the particles were helical. Structures changed significantly when pH increased from 11 to 13. Pore diameter of B-CMS2 was larger than B-CMS1 because the ordered level of B-CMS2 reduced. After loading indomethacin into B-CMS1 and B-CMS2 with solvent evaporation method, dissolution tests were studied. As B-CMS1 possessed well-ordered long helical channels and small pore diameter, indomethacin released gradually without burst-release. On the contrary, B-CMS2 showed burst release (more than 80% at 5 min)

Table 6
Various porous structure of NSNs originating from surfactant packing parameter g .

Schematic image of g value	Classified g values	Structures according to g values
	1/3	Micellar cubic (Pm-3n, Im-3 m, Fd-3 m) 3D-hexagonal (P63/mmc) Etc.
	1/2	2D-hexagonal (P6mm)
	1/2-2/3	Bicontinuous cubic (Ia-3d, Im-3 m, Pn-3 m)
	1	Lamellar
	—	—

because of its longer particle length, less-ordered multiple helices, higher curvature degree of helical channels and larger pore diameter [65] than B-CMS1.

In some cases, bimodal mesopores of NSNs can be formed under a certain pH conditions, which provides the prerequisites for its drug delivery regulation ability. Biomimetic synthesized bimodal nanoporous silica is one typical example as ibuprofen carrier [33]. The formation mechanism of B-BNS mainly depends on the active behavior of C_{16} -L-serine [34,63]. The nitrogen adsorption/desorption isotherm of B-BNS exhibited type IV isotherms in the relative pressure of 0.45–0.85 and 0.85–0.99, demonstrating that B-BNS belonged to meso-meso porous silica material. In simulated gastric fluid, ibuprofen loaded B-BNS displayed two phases of drug release due to large mesopores and small mesopores, respectively. As for simulated intestinal fluid medium, ibuprofen loaded B-BNS showed obviously controlled dissolution for 12 h with a burst release. The burst release (0–5 min) effect was due to the release of ibuprofen that physically adsorbed on the outer surface. In the second phase, the solvent took more time to diffuse into the small nanopores and internal curved mesoscopic channels, thus slowing down drug release for several hours. Based on above results, it can be concluded that B-BNS controlled ibuprofen release with two release phases in dissolution medium. Therefore, it is clear that drug delivery of NSNs can be regulated by controlling the pH of reaction system because pH has significant impact on porous structure of NSNs.

3.2. Stirring rate

The time period of stirring rate that lasts and the stirring rate when adding silica source and/or silane coupling agent should be paid great attention because they affect morphology and characteristics of NSNs. The time period of stirring rate was studied in the synthesis of chiral mesoporous silica with (CMS) with N-miristoyl-D/L-alanine as template and N-trimethoxysilylpropyl-N,N,N-trimethylammonium (TMAPS) as co-structure directing agent [66]. After adding TEOS and TMAPS into the solution containing the surfactant, NaOH and HCl, the mixture was allowed to react under stirring for 7–10 min in order to obtain CMS. It was found that no precipitate was obtained if the stirring time was shorter than 7 min, which was likely due to the difficulty in forming interaction between the surfactant micelles and the silica species as well as the insufficient hydrolysis and co-condensation of TEOS and TMAPS. On the other hand, if the stirring time was longer than 10 min, the particles did not have a twisted hexagonal rod-like morphology. Herein, the excess of stirring can enhance the reaction of surfactant micelles and silica species, resulting in the undesired products. Set CMS templated by C_{14} -L-Ala as another example [67]. The results showed that morphology and chiral structure clearly depended on the stirring rate. When the stirring rate was lower than 300 rpm, the CMS showed diverse morphologies (from twisted ribbon to twisted rod-like structures). It was clear that the length of hexagonal rod was in the range of several micrometers and the outer diameter of twisted rod varied within 50 to 800 nm. The morphologies of CMS became uniformly twisted rod-like with hexagonal cross-section when the stirring rate increased to 400 rpm. The length and the diameter of the hexagonal rod were decreased and increased with increasing stirring rate. However, the CMS synthesized at a rate faster than 1200 rpm showed a non-helical morphology. Obviously, the helical morphology of mesoporous silica is induced by stirring, and its size is controlled by the stirring rate. The stirring rate affects particle size possibly because silica condensation is influenced by stirring and silica frame can be different when changing stirring rate.

With these changes, the functions of various NSNs as drug carrier show differences. The study of B-CMS, which has studied pH impact, also discussed how stirring rate influenced characteristics and application of B-CMS [53]. B-CMS2 and B-CMS3 were prepared under the same pH condition ($pH = 13$) but different stirring rate when adding TEOS and APTES (B-CMS2: 800 rpm; B-CMS3: 200 rpm). The results demonstrated that when decreasing stirring rate from 800 rpm to 200 rpm but

others being constant, the particle length of carrier became extremely longer because cooperative self-assembly aggregation was controlled by stirring rate [67]. Particle length increased with decreasing stirring rate, suggesting that the particles may be broken up more easily by increasing torque [67]. The less ordered level of B-CMS3 had larger pore diameter compared to B-CMS2 according to nitrogen adsorption/desorption measurement. After loading indomethacin into B-CMS2 and B-CMS3 using solvent evaporation method, the drug release of indomethacin loaded B-CMS3 was faster than indomethacin loaded B-CMS2 due to the larger diameter of B-CMS3. So it provides another suggestion that the researchers can try to control the stirring rate during reaction process to obtain desired NSNs with further aims to regulate drug delivery.

3.3. Temperature

As an important parameter for chemical reactions, temperature can not be ignored in the synthesis of NSNs. On the one hand, hydrolysis and polycondensation rate of silica source are accelerated with increasing temperature, which can be clearly seen from the study of NS@P xerogel [68]. When using TMOS, consumption of time needed for preparing 30 mL NS@P sol at ambient room temperature was more than 24 h, while only several hours was enough for 30 mL NS@P sol to completely transform to gel state at 80 °C water bath. For another aspect, characteristics of NSNs are controlled by temperature based on the fact that temperature has impact on properties of surfactants.

For example, the enantiomeric excess (ee) of the CMS formed with different chiral N-acyl-amino acids follows a linear relationship upon temperature, the absolute ee values decrease with increasing temperature. The remarkable temperature dependence of ee can be interpreted thermodynamically by the equilibrium shift between two antipodal helical aggregates that triggered by the temperature. With the rotation of Ca-N single bond of the chiral N-acyl-amino acid, a new conformer, which is diastereomeric to the original one, is generated with altered topology around the head group. The rotational isomers, which are diastereomeric to each other relative to the chiral center, are quickly equilibrated mutually at ambient temperatures. However, the rate of equilibration decreases in the stacked micellar structure. For L-type N-acyl-amino acids, the conformer of lowest energy may possess the chiral sense upon packing, leading to left handed CMS. Obviously, the proportion of the conformer with higher energy is increased at higher temperature, leading to the low ee of CMS [63]. The ratio of right-handed and left-handed CMS is controlled either by kinetics or by thermodynamics [69]. The ee of the CMS is determined by the relative rate constant for l- and r-CMS formation or by the relative stability of l- and r-CMS, thus the definition of ee is $100\% \times [(l - r)/(l + r)]$. In this case, the differential activation free energy change, or the differential free energy change of the most critical stage is given by a common equation as follows.

$$\Delta\Delta G = -RT\ln(l/r) \quad (1)$$

where R and T represent the gas constant and temperature, respectively. The $\Delta\Delta G$ value is related to the differential enthalpy and entropy changes by the Gibbs-Helmholtz equation.

$$\Delta\Delta G = \Delta\Delta H - T\Delta\Delta S \quad (2)$$

Note that $\Delta\Delta H = \Delta H_l - \Delta H_r$ and $\Delta\Delta S = \Delta S_l - \Delta S_r$. Combining the two equations, a new equation was obtained.

$$\ln(l/r) = -\Delta\Delta H/RT - \Delta\Delta S/R \quad (3)$$

On the basis of $\Delta\Delta H$ and $\Delta\Delta S$ values of templates (C_{16} -L-Ala, C_{16} -L-Val, C_{16} -L-Ile, etc.), there is linear relationship $\Delta\Delta H = 0.305\Delta\Delta S - 3.022$, leading to equation:

$$\Delta\Delta H = \beta\Delta\Delta S \quad (4)$$

Therefore, the relationship between $\ln(l/r)$ and $\Delta\Delta H$ is:

$$-RT\ln(l/r) = (1 - T/\beta)\Delta\Delta H \quad (5)$$

When the temperatures equal to β , changes of $\Delta\Delta H$ never affect the $\Delta\Delta G$. What is more important, it is obvious that helical handedness of CMS can be regulated by temperature [69]. Furthermore, temperature also affects structures of ordered mesoporous silica nanoparticles, including SBA-15, SBA-16 and MCM-41. As seen from Table 7, the pore sizes of SBA-15 can be increased by enhancing the preparation temperature. The reason for the pore enlargement phenomenon at high temperature ascribes to the fact that the PEO blocks of polymer surfactants P123 become more hydrophobic and retract from the silicate walls in higher temperature, resulting in SBA-15 with larger pore sizes and thin walls [70]. Similarly, it was reported that MCM-41 synthesized at higher temperature also had larger pore diameter, possibly due to the less stability of micelles originating from the improved critical micelle concentration of CTAB in higher temperature [70]. In the structure of SBA-16 using F127 as template, the cores of spherical micelles are constituted by PO n blocks, whereas the micelle corona that consists of EO m blocks interacts with the silica framework. At lower temperature, EO m blocks are expected to favorably interact with hydrophilic silica species and have a tendency to be mixed with the silica framework. When the copolymer/silica composite is subjected to the treatment at higher temperature, these interactions become less favorable, which is expected to lead to a higher degree of aggregation of EO m blocks in the silica wall [13,71,72]. This aggregation is likely to lead to the increase in the diameter of bridges of EO m chains and resulted in pore enlargement phenomenon after removing template.

The changes of characteristics of NSNs controlled by temperature can affect drug delivery [40] (see Fig. 4). In one recent literature, two types of SBA-15 were synthesized at 60 °C and 90 °C, which were named SBA-15-B and SBA-15-A, respectively. With the influence of temperature, SBA-15-A (7.3 nm) had higher pore diameter than SBA-15-B (4.4 nm). Fenofibrate was loaded into SBA-15-A and SBA-15-B using solvent deposition method. The void space of the silica materials used in this study was filled to a greater extent, and thus the formation of amorphous fenofibrate is promoted. As a result, the drug dissolution of fenofibrate loaded SBA-15-A was faster than fenofibrate loaded SBA-15-B. What was more, in vivo results were largely in agreement with in vitro results, demonstrating that SBA-15 with larger pore diameter due to higher synthesized temperature had faster drug release rate and thus higher bioavailability. If delivery behaviors of drug loaded NSNs need to be

Table 7
The influence of temperature on NSNs and its primary reason.

Ref.	NSNs	The influence of temperature on structure of NSNs	Explanation
[69]	CMS	Helical handedness of CMS can be regulated by Temperature.	According to that obtained, the chiral structure of CMS can be controlled by temperature.
[70]	SBA-15	The pore sizes of SBA-15 can be increased from 4.6 to 11.4 nm by increasing the preparation temperature from 70 to 130 °C. SBA-15 synthesized using microwave-assisted method with pore sizes from 6.7 to 11.4 nm in the range of temperatures from 40 to 200 °C.	PEO blocks of polymer surfactants P123 become more hydrophobic and retract from the silicate walls at higher temperature.
[70]	MCM-41	MCM-41 synthesized at higher temperature had larger pore diameter.	Template micelles become less stable due to the improved critical micelle concentration of CTAB in higher temperature.
[71]	SBA-16	SBA-16 synthesized at higher temperature had larger pore diameter.	EO m blocks of F127 are less favorable to interact with hydrophilic silica species, which is expected to lead to a higher degree of aggregation of EO m blocks in the silica wall.

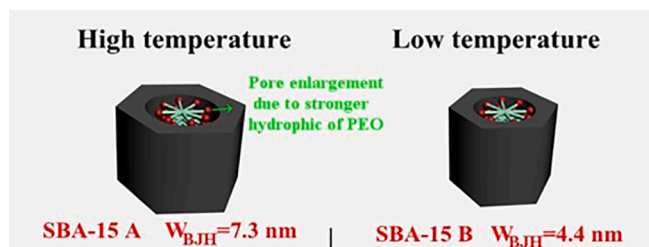


Fig. 4. Schematic abstract of how temperature influenced formation mechanism, microstructure and drug delivery of SBA-15.

regulated to improve application, temperature can be seriously considered based on its impacts on the porous structure of NSNs.

3.4. Mixture ratio

The mixture ratios of reaction materials can be the determined factor for the success of NSNs and even the regulation of NSNs with expected porous structure. The ratio of co-structure directing agent and template can be the instructor of anionic templated NSNs. The high quality of chiral structure only appears when the APTES/ C_{14} -L-AlaS molar ratio is in the range of 0.8–1.2. Larger or smaller APTES/ C_{14} -L-AlaS ratios lead to non-helical (spherical or irregular) particles [67]. Another, the NSNs can be formed only when the TMAPS/ C_{16} -L-Ala molar ratio is within the range of 0.2–0.8 to get NSNs with various structures, including lamellar, bicontinuous Ia-3d, 2D hexagonal p6mm and chiral mesophase. By packing the mesoages with different sizes and shapes, diverse mesostructures can be obtained by controlling the mixture ratio of anionic template NSNs. A full-scale synthesis-field diagram was obtained by varying the mixture ratio of TMAPS/ C_{14} GluA. Mesostructure of Fm3m, P4mm, P6mm, Pn3m and Fd3m are fabricated when the molar ratio falls into a certain range [62]. For surface modified NSNs synthesized using silane coupling agents, it has been discovered that molar ratio of silane coupling agent/(silane coupling agent + silica source) is the dominant parameter for controlling porous structure [73]. Take carboxyl modified MSU prepared by CPTES as an example, the three types of carboxyl modified MSU were synthesized, named MSU-1, MSU-2 and MSU-3 based on the molar of CPTES 0.05, 0.15 and 0.20, respectively. The results confirmed that the pore diameter, pore volumes and specific surface areas of the modified samples were observed to be dependent on the molar ratio of CPTES/(CPTES + TEOS), and the pore textural parameters decreased with increasing molar ratio of CPTES/(CPTES + TEOS) in the synthesis mixture [24]. The molar ratio of silane coupling agent/(silane coupling agent + silica source) controlled porous structure of MSU because silica condensation process was largely affected by this molar ratio.

In the aspect of drug delivery application, mixture ratio of reaction materials can impact drug release behavior of NSNs by controlling its porous structure. It has reported that a series of NSNs with different macropores and mesopores that named PMS [44] were synthesized and to investigate their delivery behavior. PEO of 0.9, 1.0 and 1.2 g was added into the reaction to obtain PMS with different porous structures, which were designated as PMS-09, PMS-10 and PMS-12, respectively. Since PEO was present, it induced phase separation of the system during the gelation, leading to the formation of bicontinuous phases. After calcination, the solvent evaporated and macroporous silica was obtained. It has been widely accepted that increasing the PEO content can retard the phase separation while has little influence on the sol–gel transition, indicating that the porous structures of the PMS can be controlled by altering the PEO content in the reaction. The following calcination removed PEO, leaving pores within the silica frame. Therefore, the sizes of the skeleton pores can be tuned via changing the PEO. The macropore diameters decreased in the order of PMS-09 (1.7 nm), PMS-10 (1.2 nm) and PMS-12 (0.7 nm) while the mesopore diameters

increased in the order of PMS-09 (3.6 nm), PMS-10 (4.1 nm) and PMS-12 (6.5 nm). For nimodipine loaded PMS, in vitro release results revealed that the drug release speed decreased in the order of PMS-09, PMS-10 and PMS-12. Since the macropores were penetrable, dissolution media can penetrate the carriers through these macropores. In this case, the contact between the drug and dissolution medium was enhanced. Consequently, the release was accelerated. In addition, hydrophobic modified MCM-41 as carrier of ibuprofen was synthesized using co-condensation method with diethoxydimethylsilane (DEDMS) as silane coupling agent [54]. The pre-mixture of DEDMS and TEOS was added into the surfactant solution under vigorously stirring. DMS-modified MCM-41 was obtained after removing CTAB. C-M41-10, C-M41-20 and C-M41-30 represented the samples that synthesized with a ratio of DEDMS: (TEOS + DEDMS) = 1:10, 2:10 and 3:10, respectively. The results revealed that pore diameters of DMS-modified MCM-41 (C-M41-10: 25 nm; C-M41-20: 2.3 nm; C-M41-30: 2.1 nm) decreased with increasing the molar ratio of DEDMS/(TEOS + DEDMS), indicating that the functional groups were on the pore surface. In the case of the C-M41-10, 60 wt% of the impregnated ibuprofen released after 1 h of assay, whereas the C-M41-20 and the C-M41-30 required almost 10 and 20 h to reach that percentage respectively, suggesting that the drug delivery rates decreased with increasing DMS modification. Therefore, mixture ratio may make contribution in constructing expected drug loaded NSNs owing to its strong power of controlling porous structures of NSNs.

3.5. Additive agents

In addition to the parameters that control characteristics of NSNs frame, including pH, stirring rate, temperature and mixture ratio, the additive agents that involved in the synthesis of NSNs should not be ignored due to their contribution in affecting porous structure of NSNs and thus regulating drug delivery. Herein, the additive agents are normally divided into surface modification and swelling agents.

3.5.1. Surface modification

In general, functional groups of NSNs are provided to change the interaction forces between drug and carriers mainly due to conversion of surface charges (such as positive charges of amino groups and negative charges of carboxyl groups) or endow the extra functionalities to NSNs (targeting delivery like pH, redox, enzyme stimuli delivery) with further aims to regulate drug delivery. Spherical MCM-41 and SBA-15 with different particle sizes were synthesized, modified by amino groups, and studied as ibuprofen carriers [74]. Both amino modified MCM-41 (MCM-41-NH₂) and carboxyl modified SBA-15 (SBA-15-NH₂) had lower pore diameters than MCM-41 and SBA-15 corresponding, demonstrating that these functional groups occupied the pore space after being grafted onto bare silica materials. The ibuprofen release equilibrium rates of MCM-41 were much faster than that of MCM-41-NH₂. The reason was that hydrogen bonding between ibuprofen and MCM-41 was relatively weak. The ibuprofen dissolution through the channels is controlled by diffusion. However, the formed COO⁻-NH₃ bond between ibuprofen and MCM-41-NH₂ was stronger than parent MCM-41, making contributing for slower drug dissolution. Another possible explanation of lower release rate could be the narrower pore diameter of MCM-41-NH₂. In a similar way, modification of SBA-15 with APTES resulted in blocking the micropores where a part of silanol groups were located. Therefore, in vitro dissolution of ibuprofen loaded SBA-15-NH₂ showed slower release behavior than parent SBA-15.

Two types of hydrophobic modified PMS (PMS-10-C₈ and PMS-10-C₁₈) were fabricated using post grafting method with C₈-triethoxysilane and C₁₈-triethoxysilane as silane coupling agents correspondingly [44]. Nimodipine was loaded into PMS, PMS-10-C₈ and PMS-10-C₁₈ using solvent soaking method. In vitro dissolution result displayed that nimodipine release speed decreased in the order of PMS-10, PMS-10-C₈ and PMS-10-C₁₈, which may be ascribed to the increase in hydrophobicity of the carriers. The hydrophobic particles can strongly attract

hydrophobic nimodipine. Since PMS-10-C18 was the most hydrophobic among these carriers, it attracted nimodipine strongest and thus resulted in the slowest nimodipine release. The results implied that altering the surface of the PMS is an efficient way to regulate drug delivery.

As for surface modified NSNs applied in delivering antitumor drugs, distinctive drug delivery effects (such as targeting delivery) can be achieved [56,75–80]. For instance, with the aim to administer drugs toward target tissues, pH sensitive molecules have been introduced to prepare surface modified NSNs. The pore surface and opening of NSNs have been functionalized with stimuli-responsive groups, inorganic nanoparticles, and peptide that worked as caps and gatekeepers. Controlled release of encapsulated drugs can be triggered in responding to internal or external stimuli such as pH, temperature, redox and enzymatic reactions. Typical examples include folate coating [77] and PEG modification [81,82]. It is worthy to address that most of the targeting delivery of antitumor drug loaded surface modified NSNs are intravenous administered. Under such circumstances, the cellular uptake of drug loaded surface modified NSNs is the prerequisite of delivering drugs to targeting sites. Therefore, it is suggested that the intake of drug loaded surface modification of NSNs by tumor cells should be paid great attention besides the performance of drug release in tumor cells.

It has been shown that the uptake of NSNs is energy-dependent by the use of metabolic inhibitors and by following the uptake at low temperature. Though there are no known cell surface receptors for silica, the uptake of MSNs has been found to take place mainly through a clathrin-coated endocytosis pathway and pinocytosis pathway, particularly for some of the surface functionalized NSNs [83]. By decorating the external surface of NSNs with different functionalities, uptake efficiency of NSNs and their ability to escape endosomal compartments can be controlled. Ionic NSNs with high surface charges can easily escape endosomal entrapment by managing the surface charge property (zeta potential) of NSNs. It has been discovered that clathrin pits can be considered as the main cell entry pathway for non-functionalized NSNs. Amine and guanidinium functionalized NSNs enter cells by a clathrin and caveolae independent mechanism, while receptor grafted NSNs depend on receptor-mediated endocytosis pathway. Therefore, functional groups for modifying NSNs in antitumor application can influence drug delivery by controlling cellular uptake mechanism and surface charges, which needs to be considered when constructing drug delivery systems.

3.5.1.1. Molecular/supramolecular switches. The marriage of molecular/supramolecular switches and NSNs endows intelligent functions to NSNs, which has great significance on regulation of drug delivery [85,86]. One drug delivery system of pH and glutathione dual-responsive MSNs (MSNs@DOX@CB) [87] was established by grafting dynamic cross-linked supramolecular network named EDA-PGOHMA and molecular switch of disulfide bonds on the surface of MSNs. The supramolecular network was formed by organizing poly(glycidyl methacrylate)s (PGMAs) chains by protonated ethanediamine (EDA) and cucurbiturils (CB). The complex of EDA and CB was achieved through cation–dipole interaction. The drug release curves of MSNs@DOX@CB in PBS with different pH (pH = 7.4, 5.0, 4.0, 3.0 and 2.0, respectively) were studied by UV spectra. According to the results, EDA-PGOHMA chains grafted on MSNs have been tightly combined by CB and effectively avoided the drug leakage. When lowering the pH value, the concentration of hydronium ions increased. In this case, it had stronger ability to bind with CB, leading to partial disassembly of the cross-linked supramolecular. Then drug released and performed pH-responsive delivery. Apart from the pH stimulus-responsive ability, the cross-linked network can be also activated by glutathione owing to its redox ability toward disulfide bonds on the polymer chains. It showed that tightly cross-linked of supramolecular network prevented glutathione from entering the inner region of polymer layer in pH 7.4 medium. On the contrary, the cross-linked supramolecular network

displayed loosened and glutathione entered into the interior of polymer layer in pH 5.0, resulting in a little DOX release. At pH = 3.0, the cross-linked network changed its shape and DOX molecules escaped from MSNs.

3.5.1.2. Biofilm on the outside layer. On the basis of silica frame, the coating of biofilms originating from lipid bilayer or cells onto NSNs affects the regulation of drug delivery (see Fig. 5). The protocells can adsorb combinations of various drugs (quantum dots, small molecules and oligonucleotides) into their nanoporous silica cores with reversible binding to the NSNs to improve drug loading capacity, thus reducing drug leakage. It has reported that the anticancer drug celastrol was loaded into MSNs and subsequently coated with a lipid bilayer. During this process, another anticancer drug axitinib, a small molecule tyrosine kinase receptor inhibitor, was encapsulated into the lipid bilayer to construct protocell ACML [88]. The MSNs were prepared using CTAB as template, TEOS as silica source and NH_4F as agent to adjust the pH of system. The obtained MSNs were spherical nanoparticles with diameter around 50 nm. ACML exhibited significant pH-responsive delivery of axitinib and celastrol because the lipid shell disassembled in acetate-buffered saline (pH 5.0) while prevented the release of encapsulated compound in PBS (pH 7.4). Therefore, drug delivery can be well regulated through coating with lipid bilayer membrane based on the mesoporous structure of MSNs. With such combination delivery of axitinib and celastrol, ACML performed effects of mitochondrial survival inhibition, drug accumulation enhancement in the cytoplasm, anti-angiogenic and mitochondrial apoptotic effects promotion. Moreover, the in vivo results confirmed that the tumor inhibitory effect. The study of coating lipid membrane onto NSNs stretches from lipid bilayer to living cells. Biomimetic strategy endows the NSNs with new and improved functionalities through applying biological membrane. A drug delivery system established by a magnetic iron oxide MSNs that coated with cracked cancer cell membranes was studied [89]. After intravenously administrating MNP@DOX@H22 into two mouse model (H22 tumor on the left hind limb and UM-SCC-7 tumor on the right), both the in vivo living fluorescence imaging and the in vivo fluorescence imaging evidently indicated the significant DOX accumulation in the H22 tumor compared to the fluorescence intensity in UM-SCC-7 tumor. Interestingly, the self-targeting to UM-SCC-7 tumor can be achieved by designing H22 cell membrane with human UM-SCC-7 cell membrane around the MNP@DOX. This discovery provides the hint that the wrapping of biological membrane may regulate drug delivery with the smart targeting effect.

3.5.2. Swelling agents

Swelling agents are used in the synthesized process with aims to enlarge pores or fabricate hierarchical nanoporous silica. It is an important determined factor of porous structure of as-synthesized products, which can certainly regulate drug delivery. Hierarchically nanoporous silica SBA-1 was successfully fabricated by employing organic mesomorphous complexes of polyelectrolyte (poly(acrylic

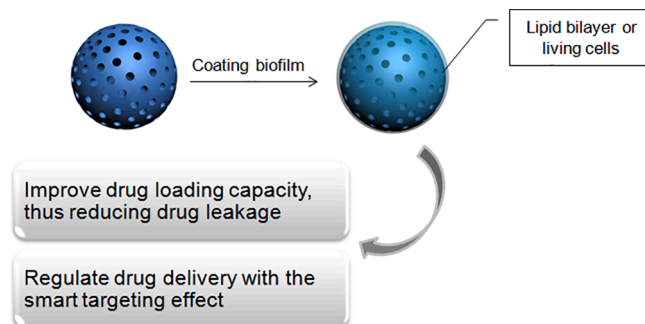


Fig. 5. Advantages of coating biofilm onto NSNs.

acid)) and cationic surfactant (hexadecylpyridinium chloride) [28]. The materials had bimodal nanopores owing to surfactant micelles and poly (acrylic acid). With the uses of 1,3,5-trimethylbenzene as swelling agent, the mesopore size of SBA-1 could be easily tuned from 3.0 nm to 5.0 nm, and the secondary nanopore were enlarged with no change of particle morphology. The result demonstrated that the addition of 1,3,5-trimethylbenzene swelled both surfactant micelles and poly(acrylic acid) phase with the aid of hexadecylpyridinium chloride.

The changed porous structure induced by swelling agents can further regulate drug delivery. It has been reported that carboxylated MSNs was synthesized using CTAB as template and dimethylhexadecylamine as swelling agent [84]. Pore-expanded carboxylated MSNs had larger pore diameter (3.5 nm) than non-pore-expanded carboxylated MSNs (2.7 nm). After incorporating trypsin inhibitor into the two carriers, the total cumulative release was 60% for pore-expanded carboxylated MSNs, but only 42% for carboxylated MSNs with non-expanded pores. For another example, face-centered cubic mesoporous silica (FMS) was prepared using F127 as template and 1,3,5-trimethylbenzene as a pore enlargement agent, and three types of FMS were obtained with different temperatures (15 °C, 18 °C and 20 °C). It showed that FMS-15, FMS-18 and FMS-20 had different pore sizes (approximately 16.0, 6.9 and 3.7 nm, respectively), demonstrating that pore diameters of FMS decreased with increasing temperature [45]. As the reaction temperature decreased, the micelle bonds were weakened, allowing more pore enlargement agent 1,3,5-trimethylbenzene to be embedded in the micelle core, thus causing pore enlargement. Celiprolol was incorporated into FMS samples (FMS-15, FMS-18 and FMS-20) by the solvent deposition method. It turned out that the cumulative release amounts within 60 min in the order: FMS-15, FMS-18 and FMS-20. This was consistent with their pore size. It can be concluded that the release behavior of celiprolol was mainly influenced by the pore size of the FMS samples. The first reason was that larger pores provided enough space and therefore less diffusion resistance for drugs to release. The second reason can be ascribed to the fact that diffusion-controlled process. Hence, functional groups or swelling agents can possibly favor the design of drug loaded NSNs with expected application in pharmaceutical field on the basis of their mechanisms in regulating porous structure of NSNs. In summary for the above critical parameters, it is a novel insight to propose that these factors can be managed mainly based on their impacts on porous structure of NSNs to design drug loaded NSNs with expected application (Fig. 6).

4. Conclusion and outlook

In summary, we have highlighted typical and recent progress in the synthesis and drug delivery application of NSNs. Specifically, formation mechanism of NSNs, extending to particular structures and synthesized routes, is presented in detail based on a large number of literature reports. Further, the relationship between formation mechanism of NSNs, their characteristics and capacity of regulating drug delivery are elucidated, which has great significance in understanding how NSNs really work as drug delivery agents. Based on this understanding, critical parameters such as pH, stirring rate, temperature, mixture ratio and additive agents, that influence the characteristics of NSNs are intensively discussed to provide valuable scientific information for controlling the porous structure of NSNs with further aim to regulate drug delivery. Controlling the porous structure of NSNs, in combination with frontline development in molecular/supramolecular switches which may be added onto the NSNs and lipid membrane coated NSNs, significantly advanced performance in drug delivery of the composite may be obtained. This has great potential application in all kinds of therapeutics and theranostics, including anticancer treatment. The ability to design and synthesize NSNs with the capacity to have drug delivery behavior (e.g. drug release rate, bioavailability, cellular uptake etc.) as required is sure to change the way we look at drug delivery systems in the coming days. It is expected that the material provided in the current review will be of some help towards fulfilling this dream of designing need-based

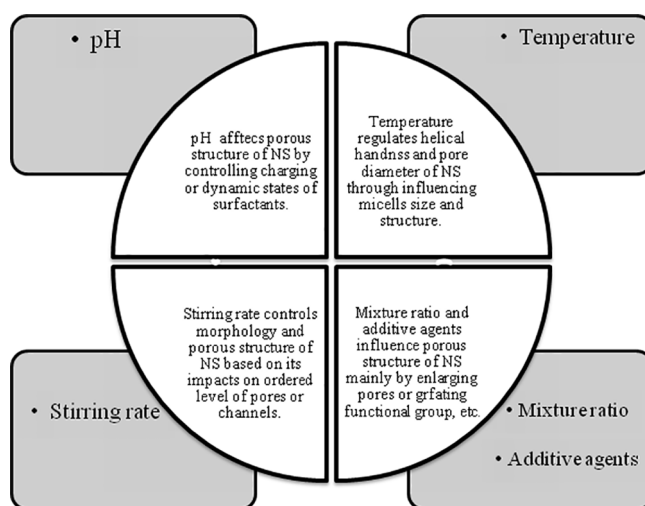


Fig. 6. Management of critical parameters for designing drug loaded NSNs.

drug delivery and reporting of action thereof. Even though such a vision may take months to be realized, all of us must work towards such a goal, especially in view of increasing demand of new and more potent pharmaceuticals every so often. This review is our contribution to this effort.

Declaration of Competing Interest

The authors declare that they have no known competing financial interests or personal relationships that could have appeared to influence the work reported in this paper.

Acknowledgements

This work has been financially supported by the Climbing Scholars from Project of Xing Liao Ying Cai of Liaoning Province in 2018 (XLYC1802055).

References

- [1] I.I. Slowing, J.L. Vivero-Escoto, C.-W. Wu, V.-S.-Y. Lin, Mesoporous silica nanoparticles as controlled release drug delivery and gene transfection carriers, *Adv. Drug Deliv. Rev.* 60 (2008) 1278–1288.
- [2] E. Verraedt, M. Pendela, E. Adams, J. Hoogmartens, J.A. Martens, Controlled release of chlorhexidine from amorphous microporous silica, *J. Control. Release* 142 (2010) 47–52.
- [3] A. Bitar, N.M. Ahmad, H. Fessi, A. Elaissari, Silica-based nanoparticles for biomedical applications, *Drug Discov. Today* 17 (2012) 1147–1154.
- [4] H. Peng, R. Dong, S. Wang, Z. Zhang, M. Luo, C. Bai, Q. Zhao, J. Li, L. Chen, H. Xiong, A pH-responsive nano-carrier with mesoporous silica nanoparticles cores and poly(acrylic acid) shell-layers: fabrication, characterization and properties for controlled release of salidroside, *Int. J. Pharm.* 446 (2013) 153–159.
- [5] S.P. Hudson, R.F. Padera, R. Langer, D.S. Kohane, The biocompatibility of mesoporous silicates, *Biomaterials* 29 (2008) 4045–4055.
- [6] K.K. Qian, R.H. Bogner, Application of mesoporous silicon dioxide and silicate in oral amorphous drug delivery systems, *J. Pharm. Sci.* 101 (2012) 444–463.
- [7] Y. Wang, N. Han, Q. Zhao, L. Bai, J. Li, T. Jiang, S. Wang, Redox-responsive mesoporous silica as carriers for controlled drug delivery: a comparative study based on silica and PEG gatekeepers, *Eur. J. Pharm. Sci.* 72 (2015) 12–20.
- [8] V. Mamaeva, C. Sahlgren, M. Linden, Mesoporous silica nanoparticles in medicine—recent advances, *Adv. Drug Deliv. Rev.* 65 (2013) 689–702.
- [9] W. Xu, J. Riikonen, V.P. Lehto, Mesoporous systems for poorly soluble drugs, *Int. J. Pharm.* 453 (2013) 181–197.
- [10] C. Charnay, S. Bégu, C. Tourné-Péteilh, L. Nicole, D.A. Lerner, J.M. Devoisselle, Inclusion of ibuprofen in mesoporous templated silica: drug loading and release property, *Eur. J. Pharm. Biopharm.* 57 (3) (2004) 533–540.
- [11] Y.-J. Cheng, G.-F. Luo, J.-Y. Zhu, X.-D. Xu, X. Zeng, D.-B. Cheng, Y.-M. Li, Y. Wu, X.-Z. Zhang, R.-X. Zhuo, F. He, Enzyme-induced and tumor-targeted drug delivery system based on multifunctional mesoporous silica nanoparticles, *ACS Appl. Mater. Interfaces* 7 (17) (2015) 9078–9087.
- [12] S. Giri, B.G. Trewyn, M.P. Stellmaker, V.-Y. Lin, Stimuli-responsive controlled-release delivery system based on mesoporous silica nanorods capped with magnetic nanoparticles, *Angew. Chem. Int. Ed.* 44 (32) (2005) 5038–5044.

- [13] M. Moritz, M. Laniecki, Application of SBA-15 mesoporous material as the carrier for drug formulation systems. Papaverine hydrochloride adsorption and release study, *Powder Technol.* 230 (2012) 106–111.
- [14] D.J. Irvine, One nanoparticle, one kill, *Nature Mater* 10 (2011) 1–5.
- [15] P.N. Durfee, Y.-S. Lin, D.R. Dunphy, A.J. Muñiz, K.S. Butler, K.R. Humphrey, A. J. Lokke, J.O. Agola, S.S. Chou, I.-M. Chen, W. Wharton, J.L. Townson, C. L. Willman, C.J. Brinker, Mesoporous silica nanoparticle-supported lipid bilayers (protocells) for active targeting and delivery to individual leukemia cells, *ACS Nano* 10 (9) (2016) 8325–8345.
- [16] E.C. Dengler, J. Liu, A. Kerwin, S. Torres, C.M. Olcott, B.N. Bowman, L. Armijo, K. Gentry, J. Wilkerson, J. Wallace, X. Jiang, E.C. Carnes, C.J. Brinker, E. D. Milligan, Mesoporous silica-supported lipid bilayers (protocells) for DNA cargo delivery to the spinal cord, *J. Control. Release* 168 (2013) 209–224.
- [17] N. Song, Y.-W. Yang, Molecular and supramolecular switches on mesoporous silica nanoparticles, *Chem. Soc. Rev.* 44 (2015) 3474–3504.
- [18] F. Tang, L. Li, D. Chen, Mesoporous silica nanoparticles: synthesis, biocompatibility and drug delivery, *Adv. Mater.* 24 (2012) 1504–1534.
- [19] B.M.N. A. R. AMILA, J. PÉREZ-PARIENTE, M.-VALLET-REGÍ, Mesoporous MCM-41 as Drug Host System, *Journal of Sol-Gel Science and Technology*, 26 (2003) 1199–1202.
- [20] P. Horcajada, A. Rámila, G. Férey, M. Vallet-Regí, Influence of superficial organic modification of MCM-41 matrices on drug delivery rate, *Solid State Sci.* 8 (2006) 1243–1249.
- [21] M. Manzano, V. Aina, C.O. Areán, F. Balas, V. Cauda, M. Colilla, M.R. Delgado, M. Vallet-Regí, Studies on MCM-41 mesoporous silica for drug delivery: effect of particle morphology and amine functionalization, *Chem. Eng. J.* 137 (2008) 30–37.
- [22] D. Zhao, J. Feng, Q. Huo, N. Melosh, G.H. Fredrickson, B.F. Chmelka, G.D. Stucky, Triblock copolymer syntheses of mesoporous silica with periodic 50 to 300 angstrom pores, *Science* 279 (1998) 548–552.
- [23] M. Nuruzzaman, M.M. Rahman, Y. Liu, R. Naidu, Nanoencapsulation, nano-guard for pesticides: a new window for safe application, *J. Agric. Food Chem.* 64 (7) (2016) 1447–1483.
- [24] Y.X. Qunli Tang, Wu Dong, Yuhun Sun, A study of carboxylic-modified mesoporous silica in controlled delivery for drug famotidine, *J. Solid State Chem.* 179 (2006) 1513–1520.
- [25] O.V. Dement'eva, I.N. Senchikhin, E.M. Sedykh, I.N. Gromyak, V.A. Ogarev, V. M. Rudy, Mesoporous SiO₂-based nanocontainers synthesized on a functional template: capacity and rate of unloading, *Colloid J* 78 (2016) 52–64.
- [26] N. Li, J.-G. Wang, H.-J. Zhou, P.-C. Sun, T.-H. Chen, Facile fabrication of hierarchically nanoporous SBA-1 nanoparticles, *RSC Adv.* 2 (2012) 2229.
- [27] N. Li, J.G. Wang, J.X. Xu, J.Y. Liu, H.J. Zhou, P.C. Sun, T.H. Chen, Synthesis of hydrothermally stable, hierarchically mesoporous aluminosilicate Al-SBA-1 and their catalytic properties, *Nanoscale* 4 (2012) 2150–2156.
- [28] N. Li, J.-G. Wang, H.-J. Zhou, P.-C. Sun, T.-H. Chen, Synthesis of single-crystal-like, hierarchically nanoporous silica and periodic mesoporous organosilica, using polyelectrolyte-surfactant mesomorphous complexes as a template, *Chem. Mater.* 23 (2011) 4241–4249.
- [29] Ahmed Mohamed El-Toni, Aslam Khan, Mohamed Abbas Ibrahim, Joselito Puzon Labis, Gamal badr, Mansour Al-Hoshan, Shu Yin, Tsugio Sato, Synthesis of double mesoporous core-shell silica spheres with tunable core porosity and their drug release and cancer cell apoptosis properties, *J. Colloid Interface Sci.* 378 (2012) 83–92.
- [30] F.S. Xiao, L. Wang, C. Yin, K. Lin, Y. Di, J. Li, R. Xu, D.S. Su, R. Schlogl, T. Yokoi, T. Tatsumi, Catalytic properties of hierarchical mesoporous zeolites templated with a mixture of small organic ammonium salts and mesoscale cationic polymers, *Angew. Chem. Int. Ed.* 45 (2006) 3090–3093.
- [31] M. Choi, R. Srivastava, R. Pyoo, Organosilane surfactant-directed synthesis of mesoporous aluminophosphates constructed with crystalline microporous frameworks, *Chem. Commun.* (2006) 4380–4382.
- [32] Z. Zhang, Y. Han, F.-S. Xiao, S. Qiu, L. Zhu, R. Wang, Y. Yu, Z. Zhang, B. Zou, Y. Wang, H. Sun, D. Zhao, Y. Wei, Mesoporous aluminosilicates with ordered hexagonal structure, strong acidity, and extraordinary hydrothermal stability at high temperatures, *J. Am. Chem. Soc.* 123 (2001) 5014–5021.
- [33] J. Li, L. Xu, N. Zheng, H. Wang, F. Lu, S. Li, Biomimetic synthesized bimodal nanoporous silica: bimodal mesostructure formation and application for ibuprofen delivery, *Mater. Sci. Eng., C* 58 (2016) 1105–1111.
- [34] J. Wang, Q. Xiao, H. Zhou, P. Sun, B. Li, D. Ding, T. Chen, Radiolaria-like silica with radial spines fabricated by a dynamic self-organization, *J. Phys. Chem. C* 111 (2007) 16544–16548.
- [35] D.J. Macquarrie, D.B. Jackson, Aminopropylated MCMs as base catalysts: a comparison with aminopropylated silica, *Chem. Commun.* (1997) 1781–1782.
- [36] C.-Y. Lai, B.G. Trewn, D.M. Jeftinija, K. Jeftinija, S. Xu, S. Jeftinija, V.S.Y. Lin, A mesoporous silica nanosphere-based carrier system with chemically removable CdS nanoparticle caps for stimuli-responsive controlled release of neurotransmitters and drug molecules, *J. Am. Chem. Soc.* 125 (2003) 4451–4459.
- [37] D.R. Radu, C.-Y. Lai, K. Jeftinija, E.W. Rowe, S. Jeftinija, V.S.Y. Lin, A polyamidoamine dendrimer-capped mesoporous silica nanosphere-based gene transfection reagent, *J. Am. Chem. Soc.* 126 (2004) 13216–13217.
- [38] J. Li, L. Xu, B. Yang, H. Wang, Z. Bao, W. Pan, S. Li, Facile synthesis of functionalized ionic surfactant templated mesoporous silica for incorporation of poorly water-soluble drug, *Int. J. Pharm.* 492 (2015) 191–198.
- [39] Y. Hu, Z. Zhi, Q. Zhao, C. Wu, P. Zhao, H. Jiang, T. Jiang, S. Wang, 3D cubic mesoporous silica microsphere as a carrier for poorly soluble drug carvedilol, *Microporous Mesoporous Mater.* 147 (2012) 94–101.
- [40] R.M. Michiel Van Speybroeck, Raf Mols, Thao Do Thi, Johan Adriaan Martens, Jan Van Humbeeck, Pieter Annaert, Guy Van den Mooter, Patrick Augustijns, Enhanced absorption of the poorly soluble drug fenofibrate by tuning its release rate from ordered mesoporous silica, *Eur. J. Pharm. Sci.* 41 (2010) 623–630.
- [41] Y. Zhang, Z. Zhi, T. Jiang, J. Zhang, Z. Wang, S. Wang, Spherical mesoporous silica nanoparticles for loading and release of the poorly water-soluble drug telmisartan, *J. Control. Release* 145 (2010) 257–263.
- [42] Y. Zhang, J. Zhang, T. Jiang, S. Wang, Inclusion of the poorly water-soluble drug simvastatin in mesocellular foam nanoparticles: drug loading and release properties, *Int. J. Pharm.* 410 (2011) 118–124.
- [43] Y. Hu, J. Wang, Z. Zhi, T. Jiang, S. Wang, Facile synthesis of 3D cubic mesoporous silica microspheres with a controllable pore size and their application for improved delivery of a water-insoluble drug, *J. Colloid Interface Sci.* 363 (2011) 410–417.
- [44] Q.-Z.G. Zhi-Guo Shi, Yi-Ting Liu, Yu-Xiu Xiao, Xu Li, Drug delivery devices based on macroporous silica spheres, *Mater. Chem. Phys.* 126 (2011) 826–831.
- [45] W. Zhu, L. Wan, C. Zhang, Y. Gao, X. Zheng, T. Jiang, S. Wang, Exploitation of 3D face-centered cubic mesoporous silica as a carrier for a poorly water soluble drug: influence of pore size on release rate, *Mater. Sci. Eng., C* 34 (2014) 78–85.
- [46] Y. Hu, Z. Zhi, T. Wang, T. Jiang, S. Wang, Incorporation of indomethacin nanoparticles into 3-D ordered macroporous silica for enhanced dissolution and reduced gastric irritancy, *Eur. J. Pharm. Biopharm.* 79 (2011) 544–551.
- [47] B. Tzankov, K. Yoncheva, M. Popova, A. Szegedi, G. Momekov, J. Mihály, N. Lambov, Indomethacin loading and in vitro release properties from novel carboxyl coated spherical mesoporous silica nanoparticles, *Microporous Mesoporous Mater.* 171 (2013) 131–138.
- [48] L.T. Zhuravlev, The surface chemistry of amorphous silica, *Zhuravlev model Colloids Surf., A* 173 (2000) 1–38.
- [49] B.C. Hancock, M. Parks, What is the true solubility advantage for amorphous pharmaceuticals? *Pharm. Res.* 17 (2000) 397–404.
- [50] R.M. Randy Mellaerts, Jasper A.G. Jammaer, Caroline A. Aerts, Pieter Annaert, Jan Van Humbeeck, Guy Van den Mooter, Patrick Augustijns, Johan A. Martens, Increasing the oral bioavailability of the poorly water soluble drug itraconazole with ordered mesoporous silica, *Eur. J. Pharm. Biopharm.* 69 (2008) 223–230.
- [51] J.S. Qianjun He, Mesoporous silica nanoparticle based nano drug delivery systems: synthesis, controlled drug release and delivery, pharmacokinetics and biocompatibility, *J. Mater. Chem.* 21 (2011) 5845–5855.
- [52] M.H. Aziz Maleki, Dissolution enhancement of a model poorly water-soluble drug, atorvastatin, with ordered mesoporous silica: comparison of MSF with SBA-15 as drug carriers, *Expert Opin. Drug Deliv.* 13 (2) (2016) 171–181.
- [53] J. Li, L. Xu, B. Yang, Z. Bao, W. Pan, S. Li, Biomimetic synthesized chiral mesoporous silica: structures and controlled release functions as drug carrier, *Mater. Sci. Eng., C* 55 (2015) 367–372.
- [54] Q. Tang, Y. Chen, J. Chen, J. Li, Y. Xu, D. Wu, Y. Sun, Drug delivery from hydrophobic-modified mesoporous silicas: control via modification level and site-selective modification, *J. Solid State Chem.* 183 (2010) 76–83.
- [55] H. Wen, J. Guo, B. Chang, W. Yang, pH-responsive composite microspheres based on magnetic mesoporous silica nanoparticle for drug delivery, *Eur. J. Pharm. Biopharm.* 84 (2013) 91–98.
- [56] X. Zhou, W. Feng, K. Qiu, W. Wang, C. He, pH-responsive mesoporous silica nanocarriers for anticancer drug delivery, *J. Control. Release* 172 (2013) e22–e23.
- [57] J. Ambati, A.M. Lopez, D. Cochran, P. Wattamwar, K. Bean, T.D. Dziubla, S. E. Rankin, Engineered silica nanocarriers as a high-payload delivery vehicle for antioxidant enzymes, *Acta Biomater.* 8 (2012) 2096–2103.
- [58] L. Tan, M.Y. Wang, H.X. Wu, Z.W. Tang, J.Y. Xiao, C.J. Liu, R.X. Zhuo, Glucose- and pH-responsive nanogated ensemble based on polymeric network capped mesoporous silica, *ACS Appl. Mater. Interfaces* 7 (2015) 6310–6316.
- [59] N. Han, Q. Zhao, L. Wan, Y. Wang, Y. Gao, P. Wang, Z. Wang, J. Zhang, T. Jiang, S. Wang, Hybrid lipid-capped mesoporous silica for stimuli-responsive drug release and overcoming multidrug resistance, *ACS Appl. Mater. Interfaces* 7 (5) (2015) 3342–3351.
- [60] J. Zheng, X. Tian, Y. Sun, D. Lu, W. Yang, pH-sensitive poly(glutamic acid) grafted mesoporous silica nanoparticles for drug delivery, *Int. J. Pharm.* 450 (2013) 296–303.
- [61] T. Yokoi, Y. Kubota, T. Tatsumi, Amino-functionalized mesoporous silica as base catalyst and adsorbent, *Appl. Catal. A* 421–422 (2012) 14–37.
- [62] L. Han, S. Che, Anionic surfactant templated mesoporous silicas (AMSSs), *Chem. Soc. Rev.* 42 (2013) 3740–3752.
- [63] H. Qiu, S. Che, Chiral mesoporous silica: Chiral construction and imprinting via cooperative self-assembly of amphiphiles and silica precursors, *Chem. Soc. Rev.* 40 (2011) 1259–1268.
- [64] C. Gao, H. Qiu, W. Zeng, Y. Sakamoto, O. Terasaki, K. Sakamoto, Q. Chen, S. Che, Formation mechanism of anionic surfactant-templated mesoporous silica, *Chem. Mater.* 18 (2006) 3904–3914.
- [65] L. Zhang, S. Qiao, Y. Jin, L. Cheng, Z. Yan, G.Q. Lu, Hydrophobic functional group initiated helical mesostructured silica for controlled drug release, *Adv. Funct. Mater.* 18 (2008) 3834–3842.
- [66] T. Yokoi, Y. Yamataka, Y. Ara, S. Sato, Y. Kubota, T. Tatsumi, Synthesis of chiral mesoporous silica by using chiral anionic surfactants, *Microporous Mesoporous Mater.* 103 (2007) 20–28.
- [67] H. Jin, Z. Liu, T. Ohsuna, O. Terasaki, Y. Inoue, K. Sakamoto, T. Nakanishi, K. Ariga, S. Che, Control of morphology and helicity of chiral mesoporous silica, *Adv. Mater.* 18 (5) (2006) 593–596.
- [68] J. Li, L. Xu, H. Liu, Y. Wang, Q. Wang, H. Chen, W. Pan, S. Li, Biomimetic synthesized nanoporous silica@poly(ethyleneimine)s xerogel as drug carrier: characteristics and controlled release effect, *Int. J. Pharm.* 467 (2014) 9–18.
- [69] H. Qiu, S. Wang, W. Zhang, K. Sakamoto, O. Terasaki, Y. Inoue, S. Che*, Steric and temperature control of enantiopurity of chiral mesoporous silica, *J. Phys. Chem. C* 112 (2008) 1871–1877.

- [70] P. Zhang, Z. Wu, N. Xiao, L. Ren, X. Meng, C. Wang, F. Li, Z. Li, F.S. Xiao, Ordered cubic mesoporous silicas with large pore sizes synthesized via high-temperature route, *Langmuir* 25 (2009) 13169–13175.
- [71] T.-W. Kim, R. Ryoo, M. Kruk, K.P. Gierszal, M. Jaroniec, S. Kamiya, O. Terasaki, Tailoring the pore structure of SBA-16 silica molecular sieve through the use of copolymer blends and control of synthesis temperature and time, *J. Phys. Chem. B* 108 (2004) 11480–11489.
- [72] C.A. McCarthy, R.J. Ahern, R. Dontireddy, K.B. Ryan, A.M. Crean, Mesoporous silica formulation strategies for drug dissolution enhancement: a review, *Expert Opin. Drug Deliv.* 13 (1) (2016) 93–108.
- [73] P. Korteso, M. Ahola, M. Kangas, T. Leino, S. Laakso, L. Vuorilehto, A. Yli-Urpo, J. Kiesvaara, M. Marvola, Alkyl-substituted silica gel as a carrier in the controlled release of dexmedetomidine, *J. Control. Release* 76 (2001) 227–238.
- [74] A. Szedegi, M. Popova, I. Goshev, J. Mihály, Effect of amine functionalization of spherical MCM-41 and SBA-15 on controlled drug release, *J. Solid State Chem.* 184 (2011) 1201–1207.
- [75] A. Vallés-Lluch, S. Poveda-Reyes, P. Amorós, D. Beltrán, M. Monleón Pradas, Hyaluronic acid-silica nanohybrid gels, *Biomacromolecules* 14 (2013) 4217–4225.
- [76] J.L. Limin Pan, Qianjun He, Lijun Wang, Jianlin Shi, Overcoming multidrug resistance of cancer cells by direct intranuclear drug delivery using TAT-conjugated mesoporous silica nanoparticles, *Biomaterials* 34 (2013) 2719–2730.
- [77] J. Pang, L. Zhao, L. Zhang, Z. Li, Y. Luan, Folate-conjugated hybrid SBA-15 particles for targeted anticancer drug delivery, *J. Colloid Interface Sci.* 395 (2013) 31–39.
- [78] N.Ž. Knežević, B. Trewyn, V.S.-Y. Lin, Light- and pH-responsive release of doxorubicin from a mesoporous silica-based nanocarrier, *Chem. Eur. J.* 17 (2011) 3338–3342.
- [79] L. Yuan, Q. Tang, D. Yang, J.Z. Zhang, F. Zhang, J. Hu, Preparation of pH-responsive mesoporous silica nanoparticles and their application in controlled drug delivery, *J. Phys. Chem. C* 115 (2011) 9926–9932.
- [80] Q. Zhao, J. Liu, W. Zhu, C. Sun, D. Di, Y. Zhang, P. Wang, Z. Wang, S. Wang, Dual-stimuli responsive hyaluronic acid-conjugated mesoporous silica for targeted delivery to CD44-overexpressing cancer cells, *Acta Biomater.* 23 (2015) 147–156.
- [81] M.S. Kim, J.B. Jeon, J.Y. Chang, Selectively functionalized mesoporous silica particles with the PEGylated outer surface and the doxorubicin-grafted inner surface: improvement of loading content and solubility, *Microporous Mesoporous Mater.* 172 (2013) 118–124.
- [82] J. Gu, S. Su, M. Zhu, Y. Li, W. Zhao, Y. Duan, J. Shi, Targeted doxorubicin delivery to liver cancer cells by PEGylated mesoporous silica nanoparticles with a pH-dependent release profile, *Microporous Mesoporous Mater.* 161 (2012) 160–167.
- [83] I. Slowing, J. Viveroescoto, C. Wu, V. Lin, Mesoporous silica nanoparticles as controlled release drug delivery and gene transfection carriers, *Adv. Drug Deliv. Rev.* 60 (2008) 1278–1288.
- [84] S. Bhattacharyya, H. Wang, P. Ducheyne, Polymer-coated mesoporous silica nanoparticles for the controlled release of macromolecules, *Acta Biomater.* 8 (2012) 3429–3435.
- [85] S.F. Lee, X.M. Zhu, Y.X. Wang, S.H. Xuan, Q. You, W.H. Chan, C.H. Wong, F. Wang, J.C. Yu, C.H. Cheng, K.C. Leung, Ultrasound, pH, and magnetically responsive crown-ether-coated core/shell nanoparticles as drug encapsulation and release systems, *ACS Appl. Mater. Interfaces* 5 (5) (2013) 1566–1574.
- [86] T. Chen, H. Yu, N. Yang, M. Wang, C. Ding, J. Fu, Graphene quantum dot-capped mesoporous silica nanoparticles through an acid-cleavable acetal bond for intracellular drug delivery and imaging, *J. Mater. Chem. B* 2 (2014) 4979.
- [87] Q.L. Li, S.H. Xu, H. Zhou, X. Wang, B. Dong, H. Gao, J. Tang, Y.W. Yang, pH and glutathione dual-responsive dynamic cross-linked supramolecular network on mesoporous silica nanoparticles for controlled anticancer drug release, *ACS Appl. Mater. Interfaces* 7 (2015) 28656–28664.
- [88] J.Y. Choi, T. Ramasamy, S.Y. Kim, J. Kim, S.K. Ku, Y.S. Youn, J.R. Kim, J.H. Jeong, H.G. Choi, C.S. Yong, J.O. Kim, PEGylated lipid bilayer-supported mesoporous silica nanoparticle composite for synergistic co-delivery of axitinib and celestrol in multi-targeted cancer therapy, *Acta Biomater.* 39 (2016) 94–105.
- [89] J.Y. Zhu, D.W. Zheng, M.K. Zhang, W.Y. Yu, W.X. Qiu, J.J. Hu, J. Feng, X.Z. Zhang, Preferential cancer cell self-recognition and tumor self-targeting by coating nanoparticles with homotypic cancer cell membranes, *Nano Lett.* 16 (2016) 5895–5901.
- [90] C.W. Wang, H.Y. Zhou, H.Y. Niu, X.Y. Ma, Y. Yuan, H. Hong, C.S. Liu, Tannic acid-loaded mesoporous silica for rapid hemostasis and antibacterial activity, *Biomater. Sci.* 6 (2018) 3318–3331.
- [91] Y. Xu, Felix Y.H. Kutsanedzie, Mehedi Hassan, Jiayi Zhu, Waqas Ahmad, Huanhuan Li, Quansheng Chen, Mesoporous silica supported orderly-spaced gold nanoparticles SERS-based sensor for pesticides detection in food, *Food Chem.* 315 (2020), 126300.
- [92] Hang Liang, Chen Jin, Liang Ma, Xiaobo Feng, Xiangyu Deng, Wu. Shuilin, Xiangmei Liu, Cao Yang, Accelerated bone regeneration by gold-nanoparticle-loaded mesoporous silica through stimulating immunomodulation, *ACS Appl. Mater. Interfaces* 11 (2019) 41758–41769.